Finite element implementation and validation of wear modelling in sliding polymer-metal contacts

F.J. Martínez[1], M. Canales[1], S. Izquierdo[1], M.A. Jiménez[1], M.A. Martínez[2]

[1]*Research, Development and Technological Services Area, Instituto Tecnológico de Aragón (ITA), María de Luna, 8 50018 Zaragoza, Spain.*

E-mail: fjmartinez@ita.es

[2]*Group of Structural Mechanics and Materials Modelling, Aragón Institute of Engineering Research (I3A), University of Zaragoza, María deLuna,3, E-50018 Zaragoza, Spain.*

Abstract

The objective of this work is to present an integral methodology to numerically model the wear phenomena by friction in a polymer-metal contact pair, showing the development of a numerical tool to implement a wear model in a commercial finite element code, Abaqus. The contact pair in which this work is based corresponds to the contact between a guide shoe insert for an elevator, made of thermoplastic polyurethane elastomers (TPU), and the corresponding guide, made of steel. Tribometer tests are planned to fit the numerically implemented wear model as well as to validate it. These tests are briefly described as an introduction to the numerical fitting of the data from which the wear model is obtained. The numerical tool in which the wear model in a polymer-steel contact pair is implemented is based on a methodology that combines the use of the user subroutine Umeshmotion, which offers the possibility of implementing a wear model in any general form, several routines to result access, and the adaptive meshing technique, a mesh smoothing tool available in Abaqus based on ALE (Augmented Lagrangian Eulerian) methods. With this technique, it is possible to eliminate material during the simulation as well as to maintain a high-quality mesh throughout an analysis by allowing the mesh to move independently of the material. As the tests that are carried out in the tribometer to fit and to validate the wear model require long travel distances and a large number of cycles, a real simulation of those tests would require a huge calculation time. Therefore, to simulate the wear process equivalent to the travelled distances in the tests in an affordable simulation time, an accelerated numerical procedure of the wear process is also proposed in this work. To numerically implement the wear model, and as it is usually stated in polymers, it is previously necessary to set up a procedure for determining the relationship between the friction coefficient and the contact pressure for the material and countermaterial contact pair. Finally, a validation of the methodology with a new wear tribometer test under different conditions to those stated to characterise the model is also presented.

Keywords: Polymer; Counterface; Wear model; Finite element simulation; Friction; Adaptive mesh

1. Introduction

The present paper presents an integral methodology to numerically model the wear phenomena by friction in a polymer-metal contact pair in order to be applied to the contact between the guide shoe insert, made of TPU, and the lift guides, made of steel, in a lift car installation. The characterisation of the wear between both parts is carried out from tribometer test results, fitting the numerically implemented wear model as well as validating it. Among all the wear types commonly present in polymers, abrasive, fatigue, erosive and adhesive wear, fatigue wear is the type involved in this case, repetitive sliding processes of TPU over steel, because this is produced against a rough counterface, with blunt projections instead of sharp projections, which could be the case of abrasion wear. In some cases, fatigue wear is also considered as abrasion wear at small scale [1][2][3].

One of the most in-depth surveys of wear modelling was carried out by Meng and Ludema [4], who catalogued over 300 wear models and equations developed over several years during the last century. They considered three main approaches to wear modelling: models based on empirical

relationships, common up to 1970 and directly constructed with data taken from tests in which few testing conditions were varied; models based on contact mechanics, common in the years 1970-1980, being models of a particular system that assume simple relationships among working conditions; and models based on material failure mechanisms, common from 1990 up to now and which include material parameters such as dislocation mechanics, fatigue properties, shear failure and brittle fracture properties. Models based on contact mechanics are the most suitable to characterise a wear model from tribometer test results. Regarding models based on empirical relationships, those are very specific to the particular characterisation test, and, on the other hand, those models based on material failure mechanisms include material parameters such as fatigue properties, shear failure or surface parameters obtained from surface characterisation techniques, so data from tribometer test results are not enough to characterise the model.

Within the models based on contact mechanics, a model of particular relevance is that proposed by Archard [5], where a linear relationship between the worn volume, the external applied load and the sliding velocity is set up by means of a specific wear rate. Despite there are some authors, like Hutchings [6], who consider that the stated expression by Archard is not suitable for polymers, it has been extensively used in literature for this type of materials. Giraldo and Vélez [7], applied the Archard equation to the study of polymers: high density polyethylene (HDPE) and nylon. Archard's model has been also used as basis for the models proposed by Liu and Li [8] and by Molinari et al. [9], who included modifications and improvements to the model proposed by Archard.

Regarding the numerical implementation of wear models, some authors consider it by taking into account the dependence of the material properties with the roughness of the countersurface [10][11]. Other authors have developed works in which the model geometry is progressively updated according to the wear model implemented to obtain realistic contact pressure distributions [12][13][14].

Another problem to solve in wear simulation of a polymer in contact with a metal countermaterial is to treat the problem of long travel distances and large number of cycles in an affordable calculation time, due to the fact that a real simulation of the wear process would require a huge amount of time. Different extrapolation schemes have been carried out by Mukras et al. [14], reducing the calculation time of the real modelling of a tribometer test by means of the proposal of using different extrapolation factors as function of the contact pressure distribution in the contact pair.

In the present study, Archard's model is taken as a first starting point to characterise the frictional wear model between TPU and steel, been characterised from tribotest results by means of a power law relationship between the volume loss and the applied load. The wear model is implemented in the Finite Element code Abaqus by means of a methodology that combines the use of the user subroutine Umeshmotion, which offers the possibility of implementing a wear model in any general form, several routines to result access, and a mesh smoothing tool available in Abaqus based on ALE methods, the adaptive meshing technique. This technique have been already used in investigations of the numerical implementation of wear processes carried out by Hegadekatte et al. [12][13] and Mukras et al. [14]. This numerical methodology carried out to numerically implement the wear process is combined with the powerful of the finite element code Abaqus to solve highly non-linear problems, such as contact phenomena and problems with high displacements and deformations, key aspect to treat with a problem of material elimination, as is the case of the wear process of a polymer-steel contact pair. Regarding the extrapolation schemes of the wear process, in the work shown in this paper, a more detailed analysis of that one presented by Mukras et al. [14] is carried out in the instant of highest contact pressure variation, and, as it will be presented in the results, of highest wear variation.

In tribology of polymers, a wide relationship can be found between friction and wear phenomena [1]. The fact of accurately characterising the friction in the contact pair is a key factor to also reproduce in a correct way the wear phenomena in the contact pair. Therefore, to take into consideration this fact, a procedure for determining a friction law relating the friction coefficient with the contact pressure between the material and countermaterial is previously set up to the wear model implementation. To do that, the relationship between the friction coefficient and the contact pressure between material and

countermaterial is considered, relationship already considered for polymers by authors such as Bouissou et al. [15].

The wear model presented in this work is developed under dry conditions given the final goal of the end-user application in the project in which this study has been carried out, which consists of the partial or total elimination of the lubricant from the application, modifying its effect by different treatments of the TPU or countermaterial surfaces [16]. Nevertheless, the methodology followed in the current work to develop a wear model by friction is not only valid for a contact pair under dry conditions, as is presented here, but also under lubricated conditions, it only being necessary to modify the way of obtaining the polymer weight loss in the wear test. However, it is necessary to bear in mind the difficulty of measuring the wear as weight loss in a wet environment, where the polymer can take up lubricant and swell, making it difficult to distinguish the effect of the polymer debris loss and that of the swelling.

The tests carried out in the tribometer to fit the wear model as well as the conditions of the real elevator require long travel distances in a large number of cycles and consequently very long testing times. Therefore, it is not reasonable from a computational time point of view to simulate the real wear process. To solve this problem, this work also includes, in addition to the numerical implementation of the wear model via the user subroutine, a procedure to simulate the wear process in an accelerated way, independently from the model meshing, and representing a compromise between accuracy of the results and computational cost. This methodology is validated with the application of the wear model to a new tribometer test of a different specimen geometry working under eccentric load conditions.

A summary of the methodology set up to numerically model the wear model is shown in Figure 1.

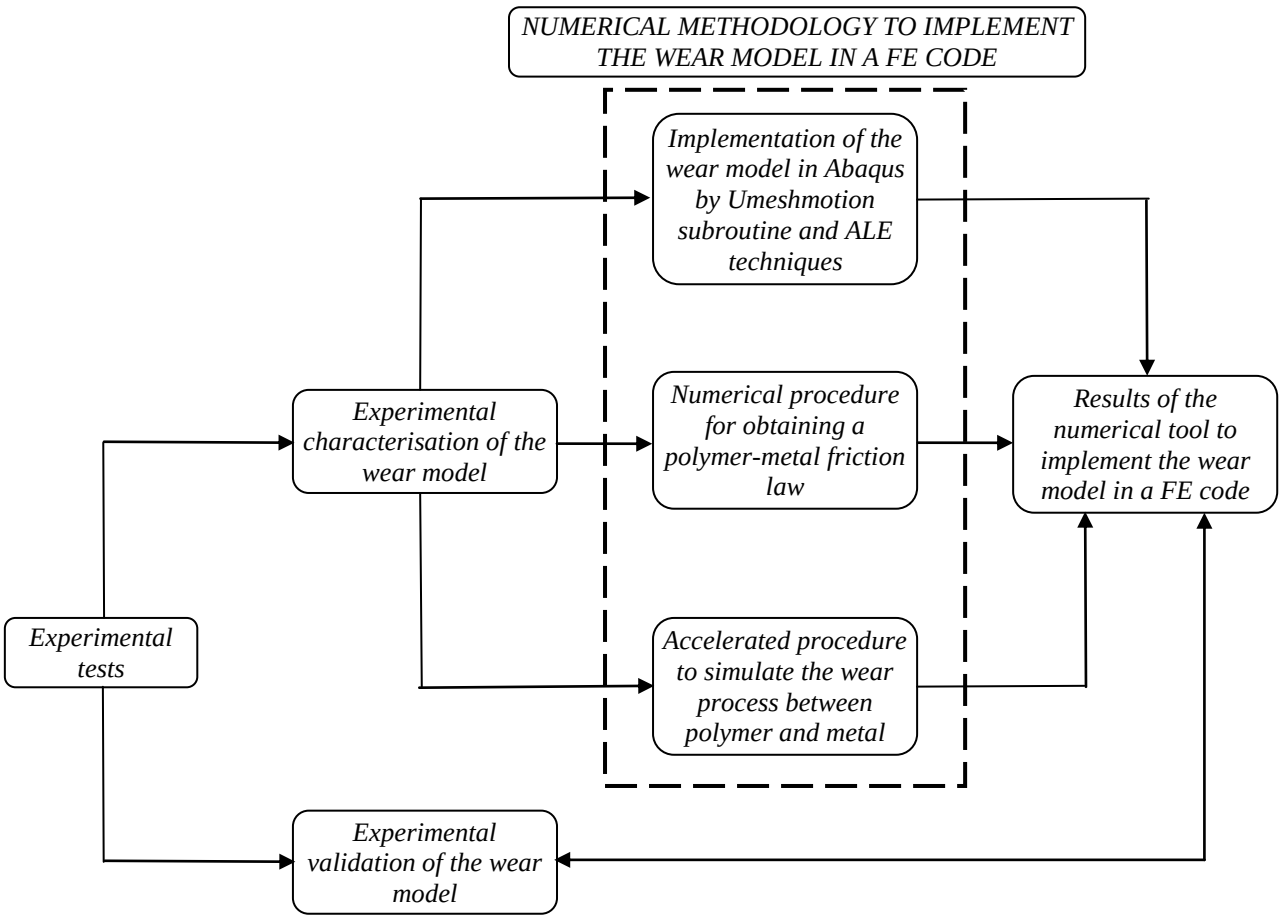

Figure 1. Methodology to numerically model the wear model in a polymer-metal contact pair.

The overall aim of this work, therefore, is to present a full methodology to numerically model the frictional wear phenomena in a polymer-metal contact pair, its implementation in the general purpose commercial finite element code Abaqus and its validation under different conditions than those stated to characterise the wear model.

2. Experimental tests

This section shows a brief summary of the tests carried out in tribometer to, firstly, characterise the wear model between TPU and steel, and secondly to validate it under different conditions to those stated in the wear test characterisation. Finally, the characterisation of the model from the results of the first set of tests is also detailed.

2.1. Experimental characterisation of the wear model

The frictional wear model implemented in this work reproduces the behaviour of a contact pair between a guide shoe insert and the corresponding guide in a lift guide shoe application. The parameters of this wear model are characterised from tribometer test data. The reciprocating flat-on-flat configuration was chosen to carry out the wear tests, considering the movement that takes place in the industrial application [17][18][19][20][21]. A TPU cylindrical specimen of 12 mm diameter and 6 mm height is extracted from the guide shoe insert and encapsulated in a steel tool of 16 mm diameter and 6 mm height in the part which encapsulates the TPU specimen and 11 mm diameter and 7 mm height at the part fixed to the machine frame. The whole acts as a moving pin, and a steel sheet extracted from the lift guide acts as a fixed counterpart. This configuration is also chosen because the counterpart sheets can be extracted from the lift car guide without geometrical limitations, as in the case of the pin-on-disc configuration. The configuration assembly and some sketches are shown in Figure 2.

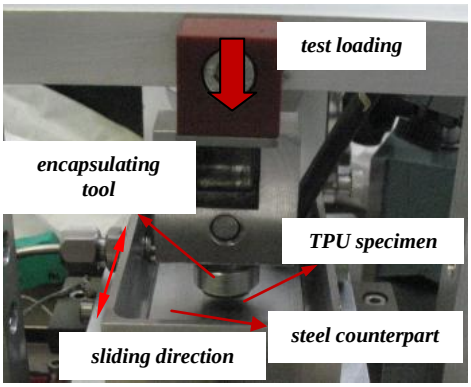

Figure 2. Assembly and sketch of the configuration in the tribometer.

The guide shoe inserts used in lift car installations are made of thermoplastic polyurethane elastomers (TPU), a material that combines the processability of thermoplastic polymers with the mechanical properties of vulcanized rubber. The properties of the material are: Young's modulus (E)= 150 MPa, yield stress (σ_Y) = 15 MPa and material hardness 48 ShoreD. Regarding its wear behaviour, this material can experience delamination and wave and melting formation as types of fatigue wear in sliding reciprocating movement. It can be treated as abrasive wear at small scale due to the asperities present in the counterface at micro level, the tensional state in the TPU being propitious to the formation of cracks at a certain depth from the material surface, which, after extension and intersection, leads to the formation of wear debris by means of sheared sheets [3][22]. Figure 3 shows an image obtained with SEM in a worn TPU sample.

The steel used as a counterpart is brushed steel of composition C 0.21%, Mn 1.5%, P 0.045%, S 0.045%, Si 0.4% and roughness between 0.8 μm and 3.2 μm. Figure 4 shows an image of the countersurface profilometry obtained with a confocal microscope during the wear test.

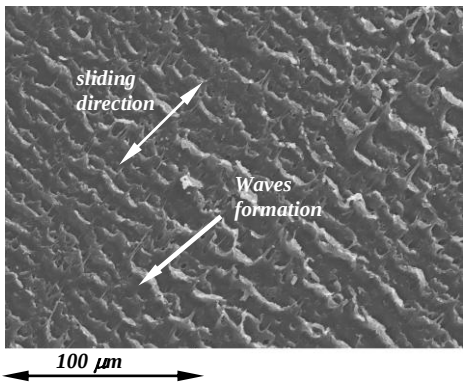

Figure 3. Image of the TPU worn surface in a reciprocating test.

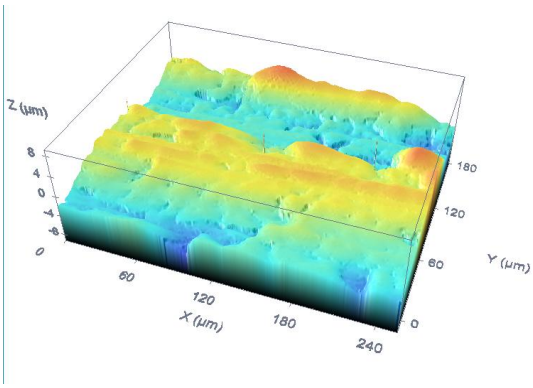

Figure 4. Steel counterface profilometry in a reciprocating test.

At the end of each test, the wear of the TPU specimen is controlled by weight loss. Apart from the specimen weight loss, it is necessary to control other parameters during the tests in order to assure their repeatability and reproducibility: the temperature in the contact pair, the counterface roughness and the presence of TPU worn debris over the counterface. The test parameters are chosen taking into account that they should if possible be within the working range of the real application. The tests are carried out at frequency 7 Hz, stroke 23 mm, temperature control between 35 ºC and 40 ºC, air blown over the counterface, preconditioning steps in load and frequency in order to set up the wear process in a smoother and more homogeneus way. Additionally, the sharpest peaks of the counterface profilometry are eliminated with a previous wear test. Regarding the test frequency, some authors have set up dependencies of this variable with the stress-strain behaviour of some polyurethanes, and although the general trend is an increase in the frequency with an increase in the material stiffness [23][24], it is not clearly related to a wear rate trend according to other investigations, where the transfer layer formation assumes an important role [19]. In the current work, all the tribotests are carried out with air blowing over the counterface in order to eliminate the TPU debris generated in the tests and put on the countermaterial surface. In relation to test frequency, even though the real application frequency remains around 0.1 Hz, the value of 7 Hz is chosen so that the whole planned test duration is reasonable, maintaining the evolution of the applied force, contact temperature and friction coefficient as stable.

The tests are carried out at normal load 50 N, 65 N, 75 N and 100 N, all corresponding to pressure values within the working range of the real application, and travel distances 500 m, 1000 m and 2500 m, values at which quantitative values of wear are attained. Between three and five repetitions are considered per condition. A more detailed description of the experimental test and the corresponding results can be found in [16].

Figure 5 shows the results of the tests in terms of volume loss.

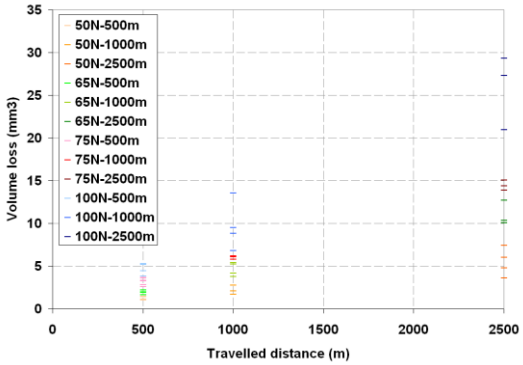

Figure 5. Volume loss along the travelled distance for the tests.

Once the tribometer tests to fit the wear model are performed, the analysis of the results dependency [11] is carried out according to Archard's model [5], shown in equation (1).

$$q = \frac{k}{H} \cdot F \cdot s \tag{1}$$

where q [mm^3] is the worn volume, F [N] the applied normal load, s [m] the sliding distance, k the non-dimensional wear coefficient particular to the contact pair characteristics and H [N/mm^2] the material hardness, the ratio k/H [$mm^3\ N^{-1}\ m^{-1}$] known as the specific wear rate. To study the relationships stated in equation (1), the dependencies between the volume loss, the travelled distance and the load applied in the tests are carried out. Both relationships are shown in Figure 6.

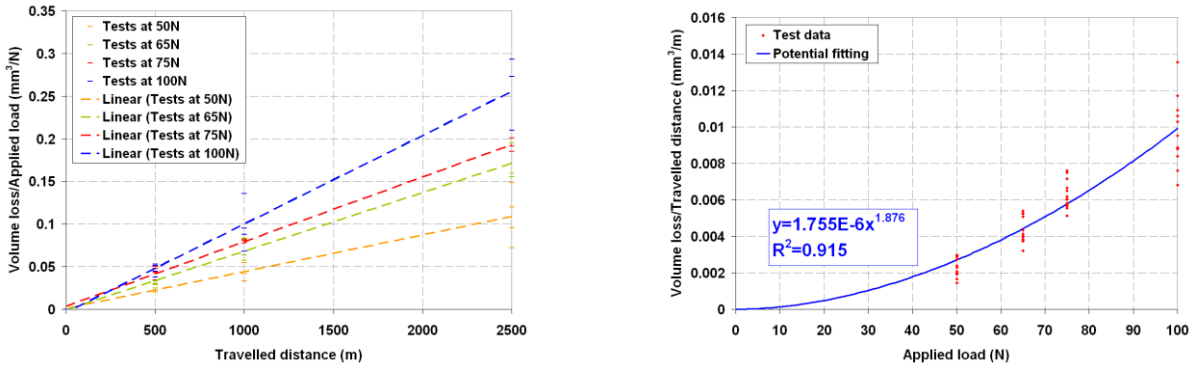

(a). Relationship between the volume loss and the travelled distance.

(b). Relationship between the volume loss and the applied load.

Figure 6. Relationships between the volume loss, the travelled distance and the applied load.

According to Figure 6, the volume loss and the travelled distance show a linear relationship, but the best fitting predicts a power law relationship between the volume loss and the load applied, contradicting what is stated by Archard's law, where the relationship is linear. According to microscopic observations carried out on the TPU worn surface and also to relationships obtained in the tensional analysis of the contact zone, both studied in a previous work [16], there is a double linear effect that leads to the non fulfilment of the linear relationship between worn volume and applied load, stated by Archard. Some authors, like Thomas et al. [25] and Cho and Lee [26], have carried out investigations in polymers about relationship between the abrasive wear mechanism and mechanical fatigue process by means of crack growth theories. In [16], this relationship is confirmed, stated that wear occurs as a result of repeated crack propagation in the subsurface layer of the material at a small scale. In order to be implemented numerically, the wear model is stated so that the volume loss is related, by means of this power law relationship, to the contact pressure instead of the applied load. Equation (2) shows the power law relationship numerically implemented.

$$q = \alpha \cdot s \cdot A \cdot \left(\frac{p}{E}\right)^{\beta} \tag{2}$$

where q [mm^3] is the wear loss, s [m] the travelled distance, A [mm^2] the contact area, p [N/mm^2] the contact pressure, α and β dimensionless constants obtained from the data fitting and E [Nmm^{-2}] the initial Young's modulus of the worn material, included in the equation to express the variables in the equation in consistent units and to avoid numerical problems in the user-subroutine compilation using fitted constants with enough significant figures. Equation (2) can also be expressed in a differential way, according to equation (3).

$$\dot{q} = \alpha \cdot v \cdot A \cdot \left(\frac{p}{E} \right)^{\beta} \quad (3)$$

with $\dot{q}\ [mm^3\ s^{-1}]$ being the rate of volume loss and $v\ [m\ s^{-1}]$ the sliding velocity. The numerical values of these parameters and the process carried out to obtain them are described in sections 3 and 4.

2.2 Experimental validation of the wear model

This section also describes the conditions of the wear test carried out to validate the wear model implemented by means of the user-subroutine. This test is planned with a specimen of geometry different to those developed for the wear model fitting, rectangular instead of cylindrical, and working under eccentric load conditions instead of centred load conditions. By this way, the objective of this validation is to study the validity or the capacity of prediction of the wear model characterised under specific conditions, and which response is evaluated under very different conditions, in geometry as well as in load. The parts involved in the system consist of a TPU specimen, with a rectangular part to establish contact with the counterpart, of dimensions 16 x 11.7 mm^2 contact surface and 6 mm height, and encapsulated in a rigid tool with a cylindrical part of 10 mm diameter and 11 mm height, which acts as a mobile pin and slides with a flat-on-flat reciprocating movement along a fixed counterpart. This rigid tool is at the same time fixed to the machine frame. The mobile pin is fixed to the machine frame by means of a screw located at half the height of the encapsulating tool. Both parts in contact are extracted from the real application: the TPU specimen from the guide shoe insert and the counterpart from the lift car guide, being the same counterpart as that used in the wear tests carried out to fit the wear model.

The methodology followed in this test is the same as that explained above in the tests to fit the wear model, with test stroke of 23 mm, control of the maximum temperature of 40ºC by the tribometer thermocouple, air blown over the countersurface at 1 bar, thermal resistance activated at 35ºC and preconditioning load and frequency steps. The test conditions are 75 N of applied load along 1000 m of travelled distance.

Figure 7 shows a sketch of the parts involved in the wear validation test.

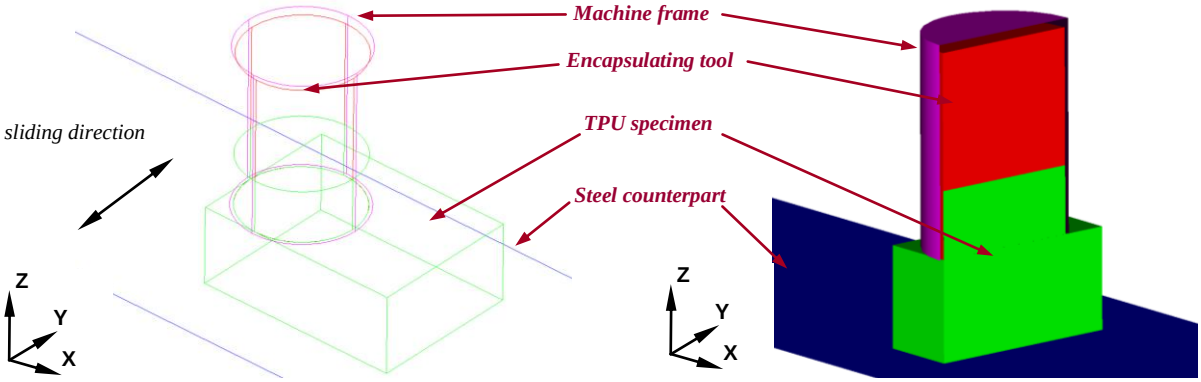

Figure 7. Sketch of the configuration of the wear model validation test (whole model and model cut by half the encapsulating tool).

Table 1 shows the results of the test in terms of specimen weight loss.

Table 1

Results of the tests to validate the wear model

Test	*Applied load (N)*	*Travelled distance (m)*	*Weight loss (g)*	*Volume loss (mm^3)*
1	75	1000	0.04223	34.31

Figure 8 shows different views of the worn surface of the TPU specimens after the test. In the first view, it is shown as the sliding direction corresponds to the vertical direction of the image, while in the rest of views, it is remarkable the decrease of thickness in the specimen.

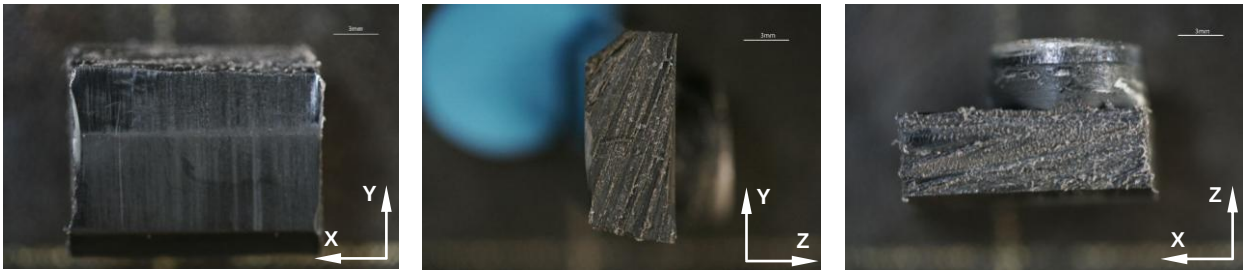

Figure 8. Worn surface of the TPU after the wear test to validate the wear model (75 N at 1000 m of travelled distance).

3. Numerical methodology to implement the wear model in a FE code

The numerical implementation of the frictional wear model between TPU and steel in a FE code, Abaqus, sets up the development of three different methodologies: firstly, the development of a tool for implementing the wear model in Abaqus, combining the use of the user subroutine Umeshmotion, for implementing the wear model obtained from tribometer test results, several routines to result access, and the adaptive meshing technique in order to eliminate the worn material and maintaining a high-quality mesh throughout the simulation. Secondly, a numerical procedure for obtaining a polymer-metal friction law due to the close relationship between friction and wear phenomena in polymers. Finally, the last procedure consists in the development of an accelerated numerical procedure to simulate the wear process in an affordable calculation time due to the long distances and large number of cycles required in a wear test, including a numerical-experimental validation under different conditions stated to characterise the wear model.

3.1. Implementation of the wear model in Abaqus by Umeshmotion subroutine and ALE techniques

Taking into consideration the dependence of the wear loss with the contact pressure obtained in the wear model detailed in equation (3), it is critical to obtain the most accurate possible evolution of the model deformed shape to obtain an accurate evolution of the contact pressure distribution. It is not enough to obtain the solution with a static calculation because the variation of the contact distribution due to material loss is not considered. This problem can be dealt with in Abaqus by implementing with the subroutine Umeshmotion the rate of material loss of equation 3, specifying the rate of material loss as ablation velocity at the nodes on the exterior surface in contact with the sliding surface. This subroutine is used in conjunction with the adaptive meshing technique, also available in Abaqus, a mesh smoothing tool applied at the end of each converged increment. This technique defines adaptive mesh constraint velocities adjusting the nodes in a defined interior region and, therefore, allowing the mesh to independently move to the material. The goal of this technique is to maintain a well-shaped mesh as the ablation velocities are specified, through the user subroutine, to the exterior nodes in contact with the sliding surface. The adaptive meshing technique combines the features of pure Lagrangian analysis and pure Eulerian analysis, often referred to as Arbitrary Lagrangian-Eulerian (ALE) analysis. It is necessary to point out that this technique is appropriate depending on the type of material for which it is applied; for instance, it performs poorly with hyperelastic material models, due to the inaccurate advection of the deformation gradient state variables. Therefore, it is recommended to model the zone where the adaptive mesh technique is applied with an elastic material definition.

To be implemented numerically, equation 3 needs to be expressed as discrete values in each node *i* of the contact surface. Thus, the equation can be expressed in a nodal way according to equation (4).

$$q_i = \alpha \cdot v_i \cdot A_i \cdot \left(\frac{p_i}{E} \right)^{\beta} \tag{4}$$

The addition of the wear in all the nodes N of the contact surface results in the total wear according to equation (5).

$$q = \sum_{i=1}^{N_{contact}} q_i \tag{5}$$

The user subroutine Umeshmotion allows the position or the motion to be specified of nodes that belong to an adaptive mesh constraint node set following the expressions shown in equation 4, calling to several utility routines available in Abaqus in order to access results data at the nodes. In this way, the rate of material loss of the nodes at the contact zone of the worn material with the countersurface is calculated by calling the variables of equation 4, that is: nodal contact pressure, nodal contact area and nodal sliding velocity. At the same time, it is necessary to specify the group of nodes to which the adaptive meshing is applied and to specify how the motion is prescribed to those nodes. The adaptive mesh technique also allows specific ablation directions to be defined at zones of the model with geometric singularities such as corners or edges, in order to maintain the model with a well shaped deformation. The fitted material constants are input to the subroutine as external variables to the model.

The process followed in the calculation with the user subroutine Umeshmotion is detailed in Figure 9.

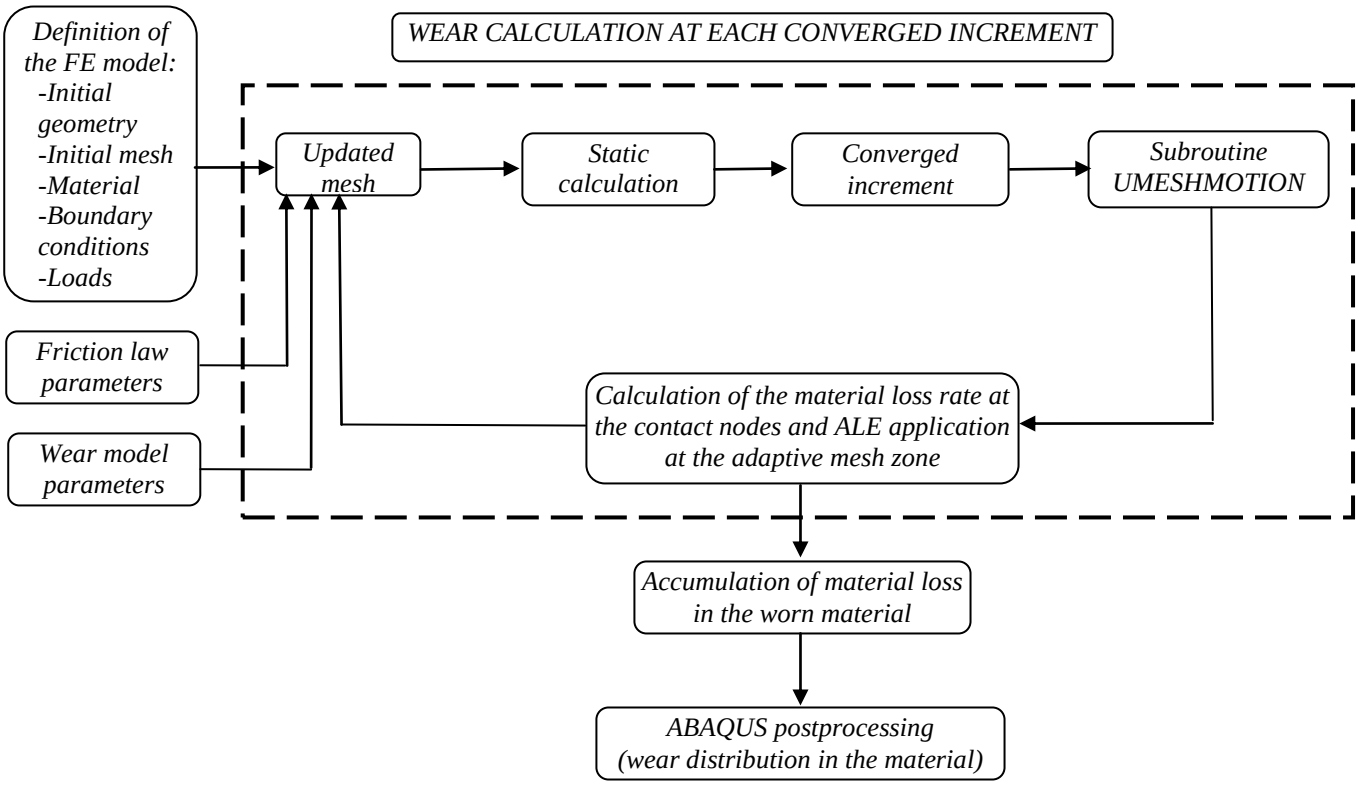

Figure 9. Calculation process with the user subroutine Umeshmotion.

The implementation of the wear model, referred to in equation 4, in the user subroutine Umeshmotion is detailed as follows in Figure 10.

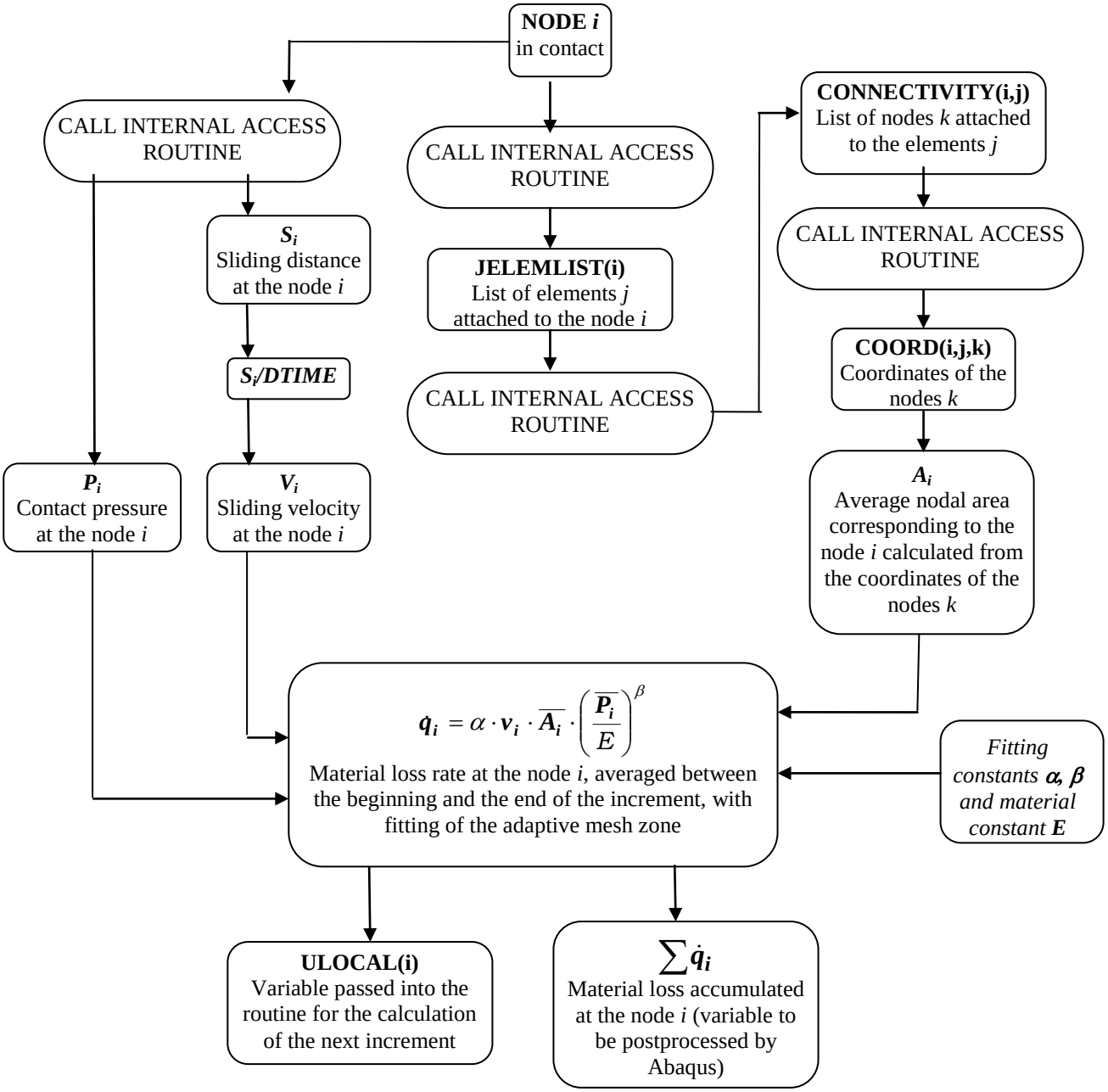

Figure 10. Implementation of the wear model for node *i* in the subroutine Umeshmotion.

3.2. Numerical procedure for obtaining a polymer-metal friction law

One of the most influential parameters in the wear phenomenon of the TPU-counterpart contact is the friction coefficient. In rubber-like materials and polymers, an important dependence of the friction coefficient with the contact pressure has been stated [15][27]. To determine this dependence, tribometer tests can be used to set up a first estimation of the mean values of both variables. However, a more detailed procedure is required to compute the actual relationship between the friction coefficient and the contact pressure due to the fact that the real contact does not correspond with the total area of the TPU specimen and the contact pressure distribution is not uniform on the base. To fit this law, a numerical fitting procedure based on a fixed-point method [28][29] is set up. This procedure is carried out with results of the finite element simulations of one cycle of the wear tribometer tests, validating this methodology with values of the friction force attained in those tests. Other methods developed in the literature for more complex contact pair geometries are based on the search of the function which best

fits the fixed data pairs [30], unlike the method carried out in this work, where the differences attained in the data pair values during the iterative process are minimised.

The fixed-point method is applied to an equation of type $g(x)=x$, considering an initial value x_0, and taking into account the formula $x_{n+1}=g(x_n)$, with $n\geq 0$. The value p is defined as:

$$p=\lim_{n\to\infty} x_n=\lim_{n\to\infty} g(x_{n-1})=g\left(\lim_{n\to\infty} x_{n-1}\right)=g(p) \tag{5}$$

Therefore, p is the solution sought in the case of there being a limit of the function and g being continuous in p. The method stops when $|x_{n+1}-x_n|$ is lower than a tolerance defined as the precision level with regard to the exact solution.

In this case, the method is developed by means of the simultaneous fitting of two variables, contact pressure and friction coefficient, which represents the friction law between material and counterpart. To begin the iterative process, the initial values are taken from data of the tests at 50N, 65N, 75N and 100N, considering, at each condition, average contact pressure calculated as the ratio between the normal force and the total specimen area in contact with the counterpart, and the friction coefficient as the ratio between the friction force attained in the tests and the normal force. To complete the friction curve, values of the friction coefficient at lower and higher contact pressures are also taken so that friction force values obtained in the simulations at each condition fit those attained in the tests at the end of the iterative process. With all these data pairs, a fitting with an exponential function is carried out to obtain an analytical expression of the friction law, which feeds, at each load condition, one cycle finite element simulations of the wear tests in the tribometer. As convergence criteria, at the end of the iterative process the total friction force values obtained in the simulations at each load condition must fit those attained in the tribometer tests. The postprocessing of each simulation gives new data pairs of contact area and of average friction coefficient, calculated as the ratio between the friction force and the normal force, at each load condition. Maintaining the same values of friction coefficient at low and high contact pressure values, a new friction curve is fitted with an exponential function, which feeds again the finite element simulations of one cycle of the wear tests. This iterative process is followed up to a level of tolerance between the data pairs of friction coefficient and contact pressure before and after one interaction, for each condition, of lower than 1%. A summary of the procedure is shown in Figure 11.

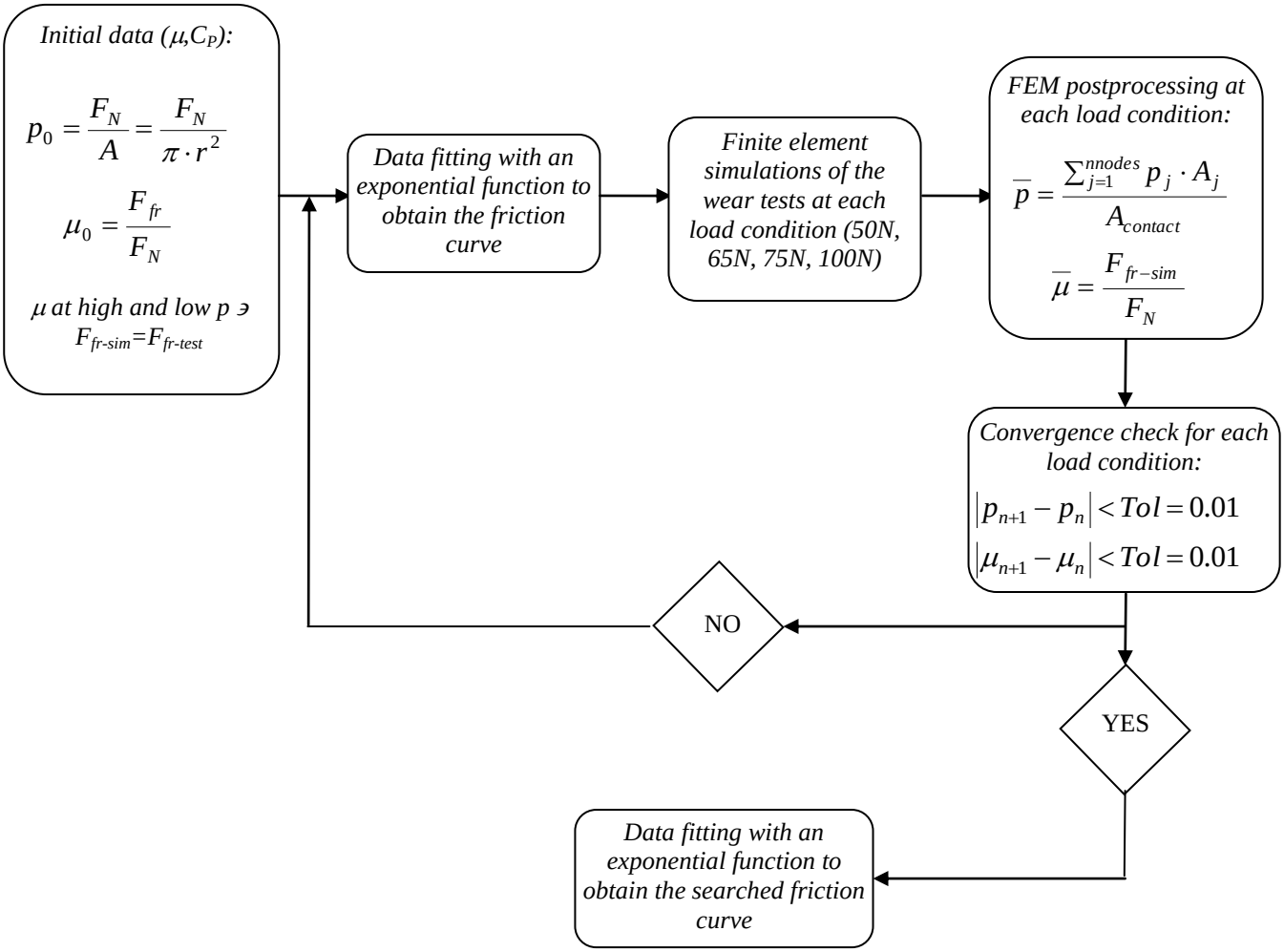

Figure 11. Fitting procedure of the material-counterpart friction law.

3.3. Accelerated procedure to simulate the wear process between polymer and metal

The tests carried out in the tribometer to fit the wear model as well as that carried out to validate it require long travel distances in a large number of cycles and consequently very long testing times. Therefore, to simulate the wear process involving long travel distances, it is necessary to set up a procedure to simulate an accelerated wear process. The fitting of the procedure is carried out by means of finite element simulations of the TPU pad wear process.

This study is performed for the case of an external load of 75 N at 1000 m of travelled distance. An equivalent procedure would be applied for the rest of external loads. This work aims to set up an analysis of the equivalent wear per cycle considering different travelled distances, studying the evolution of the wear curve along the distance. Several authors distinguish different stages to be considered in a wear process: a first running-in stage with a high wear rate in which the contact pair is set up and the microasperities of both surfaces are eliminated, a second stationary stage where a constant wear rate has been attained and the surface or surfaces are worn in a steady and uniform way and finally, a third stage in which the uniform wear is lost and the wear rate increases in an accelerated way [1][26]. Nevertheless, apart from the effect of the elimination of microasperities, the wear rate in the first stage could be also affected by the geometric modification of the specimen caused by the high friction coefficient between both parts, which implies an abrupt change in the contact pressure distribution and, as it will be shown in the results, in the wear rate.

Therefore, in order to study the first stage of the wear process accurately, the process is based on a politomic division method [31][32], in which the total travelled distance, 1000 m, is divided into several cycles, focusing a higher number of cycles in the first stage. The first simulation corresponds to only one division in which the total wear attained according to the wear model in 1000 m is applied in one cycle of simulation, that is, the constant α is multiplied by a factor of 1000/0.046, corresponding to the equivalent simulated travelled distance/real travelled distance. In the second simulation, two divisions are taken, the first with 2^1=2 cycles (equivalent travelled distance=250m in each) and the second with 2^0=1 cycle (equivalent travelled distance=500m). The third simulation is divided into three divisions, the first with 2^2=4 cycles (equivalent travelled distance=83.33m), the second with 2^1=2 cycles (equivalent travelled distance=166.67m) and the third with 2^0=1 cycle (equivalent travelled distance=333.33m). This process is followed, considering the number of cycles according to the formula 2^{n-m}, with n the number of divisions and m the corresponding subdivision, up to 10 divisions with the aim of increasing the number of steps in the running-in stage, initial wear stage, when the number of divisions increases. This number of divisions corresponds to the maximum integer number in which the wear simulated in one cycle is higher than the real experimental wear, which would correspond to 10.6 divisions. Additionally, the wear attained at the end of each simulation is compared with the mean experimental value attained in the tests, 0.0074 g, equivalent to 6.013 mm^3 (TPU density=0.00123 g/mm^3).

The results obtained with the application of this method are detailed in the section of results.b Additionally, this procedure also studies the importance of updating the geometry after applying the wear model by means of the user subroutine and the adaptive mesh technique in the wear results, the analysis of the pad mesh influence and an analysis of the TPU material model. To complete the analysis, a numerical-experimental validation of the methodology is set up with the simulation of a test under different conditions to those stated to characterise the wear model.

4. Results of the numerical tool to implement the wear model in a FE code

This section encloses the results of the methodology to implement the wear model: firstly, of the numerical procedure for obtaining a TPU-steel friction law and secondly, of the accelerated numerical procedure to simulate the wear process.

4.1. Results of the numerical procedure for obtaining a material-counterpart friction law

Figure 12 shows the results of the tribometer tests performed to analyse the dependence of the friction coefficient with the normal force, in terms of mean values of both variables.

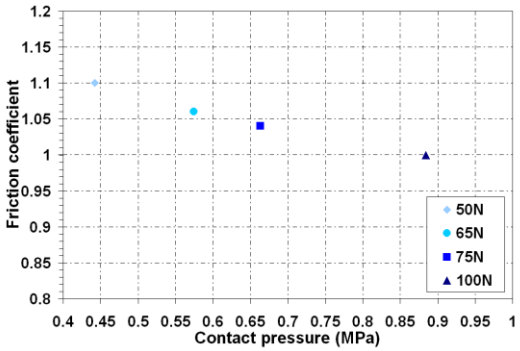

Figure 12. Mean contact pressure-friction coefficient relationship for the different load conditions.

To develop the procedure based on the fixed-point method, results from finite element simulation of one cycle of the wear tribometer tests are used, validating this methodology with values of the friction force attained in those tests. A three dimensional finite element model is built in order to reproduce the same experimental conditions set up in the tribotests. The parts considered in it are the counterpart and

encapsulating tool, considered as analytical rigid surfaces, and the TPU pad, considered as a deformable body and meshed with C3D8 elements (three dimensional elements with eight nodes per element), available in the Abaqus library. A scheme of the model with the parts involved is shown in Figure 2, while Figure 13 shows an image of the finite element model used.

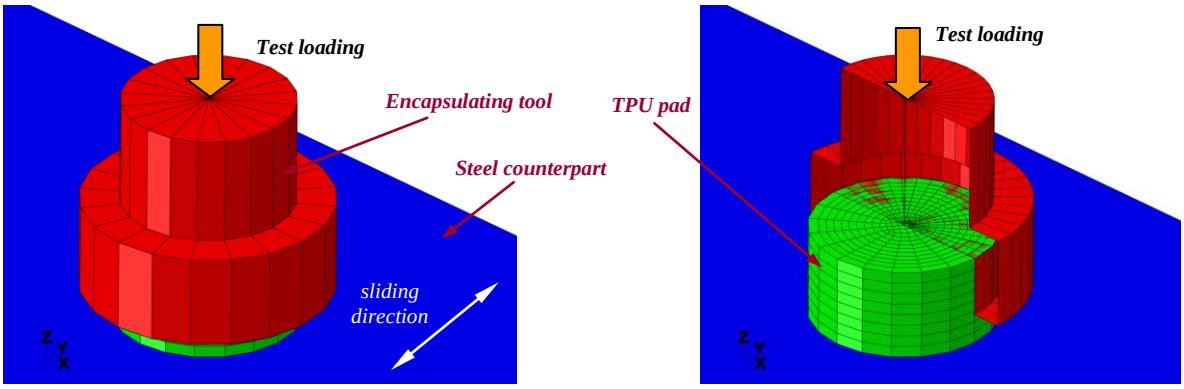

Figure 13. Finite element model of the tribotest used to obtain the material-counterpart friction law.

The TPU material properties of the pad are obtained from uniaxial tensile and compressive characterisation tests [33][34] carried out on specimens extracted from a guide shoe. Although TPU is considered as a rubber-like material in some studies [35][36], the ALE technique performs poorly with hyperelastic material models, due to the inaccurate advection of the deformation gradient state variables, as has already been commented. Considering that almost all the material belongs to the adaptive mesh zone, the whole specimen is modelled with a linear elastic material of Young's modulus 150 MPa, obtained from the material characterisation test fitting, and with a Poisson's coefficient of 0.35, a typical value obtained for this material from the literature. A further analysis of the influence of the TPU material, modelled as linear elastic and as elastoplastic, is presented in the next section. The interaction between the TPU and countermaterial is defined by the friction law to be developed with dependence between the friction coefficient and contact pressure, while the exterior nodes of the TPU pad which are in contact with the encapsulating tool are tied to it, following its movement during the simulation.

The geometry and meshing of the model is carried out using the I-DEAS code, while the software used in the calculations is Abaqus /Standard-v6.8. The model consists of 2117 nodes and 1794 elements.

The fixed-point method applied to the results of the finite element simulations sets up the simultaneous fitting of two variables, contact pressure and friction coefficient. The different iterations obtained in the fixed-point method application, detailed in section 3, give the results enclosed in Table 2.

Table 2
Variable values in the numerical fitting procedure for the material-counterpart friction law

Iteration		*Load condition (N)*								*Fitting with exponential function:* $\mu = a + b \cdot e^{-p/c}$			
		50		65		75		100		*a*	*b*	*c*	R^2
		p	μ	*p*	μ	*p*	μ	*p*	μ				
1	*Initial values*	0.4421	1.1	0.5747	1.06	0.6631	1.04	0.8842	1	0.9604	1.0385	0.2365	0.9982
	Final values	0.5954	1.0745	0.7515	1.0376	0.8678	1.0205	1.1418	0.9939	-----	-----	-----	-----
	Deviation	0.3467	0.0232	0.3076	0.0211	0.3085	0.0188	0.2913	0.0061	-----	-----	-----	-----
2	*Initial values*	0.5954	1.0745	0.7515	1.0376	0.8678	1.0205	1.1418	0.9939	0.9584	1.041	0.2863	0.9988
	Final values	0.5954	1.1017	0.762	1.0616	0.8796	1.0417	1.1418	1.0083	-----	-----	-----	-----
	Deviation	9.6E-5	0.0253	0.014	0.0231	0.0137	0.0208	4.4E-5	0.0146	-----	-----	-----	-----
3	*Initial values*	0.5954	1.1017	0.762	1.0616	0.8796	1.0417	1.1418	1.0083	0.9605	1.0384	0.3194	0.9982
	Final values	0.5991	1.1202	0.775	1.0794	0.8948	1.0584	1.1592	1.02	-----	-----	-----	-----
	Deviation	0.0062	0.0168	0.017	0.0168	0.0173	0.016	0.0152	0.0117	-----	-----	-----	-----
4	*Initial values*	0.5991	1.1201	0.775	1.0794	0.8948	1.0584	1.1592	1.02	0.9629	1.0355	0.3449	0.9975
	Final values	0.6065	1.1338	0.775	1.0929	0.8949	1.0715	1.1592	1.0329	-----	-----	-----	-----
	Deviation	0.0124	0.0121	2.3E-5	0.0125	3E-5	0.0124	4.1E-5	0.0126	-----	-----	-----	-----
5	*Initial values*	0.6065	1.1337	0.775	1.0929	0.8949	1.0715	1.1592	1.0329	0.9637	1.0344	0.3658	0.997
	Final values	0.6065	1.1433	0.7798	1.1024	0.8949	1.0808	1.1751	1.0408	-----	-----	-----	-----
	Deviation	1.7E-5	0.0084	0.0062	0.0087	4.4E-5	0.0086	0.0138	0.0076	-----	-----	-----	-----
6	*Initial values*	0.6065	1.1433	0.7798	1.1024	0.8949	1.0808	1.1752	1.0408	0.9656	1.0321	0.378	0.9964
	Final values	0.6066	1.1496	0.7798	1.1089	0.895	1.0872	1.1753	1.0467	-----	-----	-----	-----
	Deviation	1.5E-5	0.0055	3.2E-5	0.0059	4.2E-5	0.006	6.3E-5	0.0057	-----	-----	-----	-----

***The deviation is defined as:** $\frac{|p_{n+1} - p_n|}{Cp_n}$ **or** $\frac{|\mu_{n+1} - \mu_n|}{\mu_n}$**, depending on the variable.**

Graphically, Figure 14 shows the evolution of the data pairs *p*-μ and of the friction curve obtained by the fitting of the data with exponential functions.

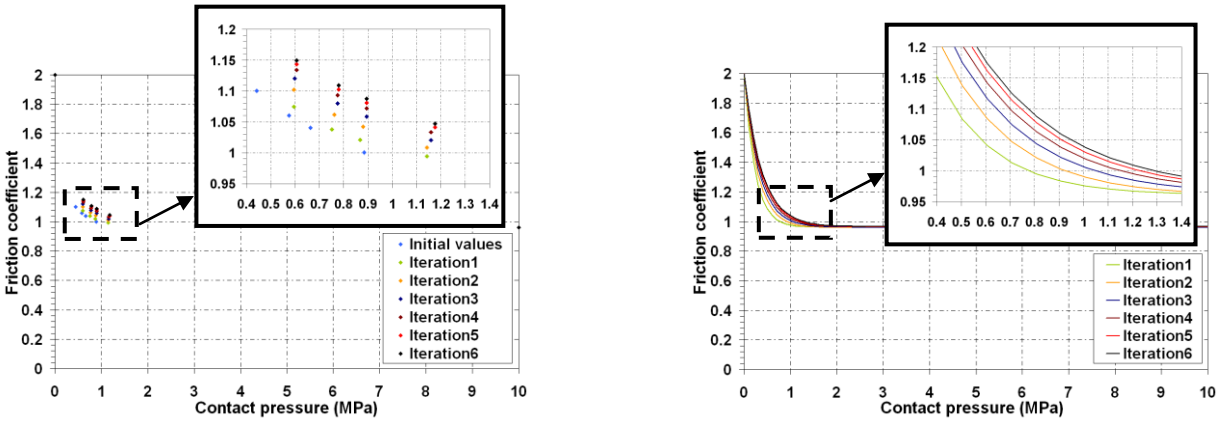

(a). Evolution of data pairs p-μ.

(b). Evolution of the friction curves.

Figure 14. Evolution of p-μ obtained in the friction law fitting procedure.

According to the results shown above, along the iterations, friction coefficient tends to increase due to contact area progressively decreases. Another conclusion is that six iterations are required to achieve a deviation lower than 1% in both variables with regard to the last deviation, p and μ. On the other hand, it should be remarked that it is necessary to extrapolate in the initial and final parts of the curve, which should be avoided in case of sharp variations in the fitting points along iterations. In this case, the fitting should be fed with a wider range of contact pressure in order to carry out a lower extrapolation.

4.2. Results of the accelerated procedure to simulate the wear process between TPU and steel

As first task, once the friction model between TPU and steel has been characterised, the fitting of the tribometer data relating the volume loss with the external force, shown in Figure 6 (b), needs to be transformed into a relationship between the volume loss and the contact pressure to be implemented numerically, as is shown in equation 2. With the values of contact pressure attained in the sixth iteration of the fitting procedure for obtaining a material-counterpart friction law, detailed in section 3.2, the fitting of equation 2 gives the following values for the dimensionless constants: α = 3.45 and β =3.5, which fitting is shown in Figure 15.

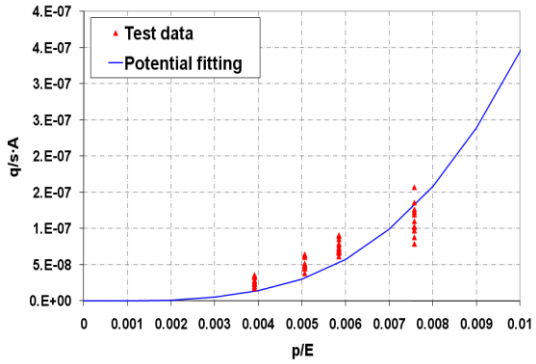

Figure 15. Relationship between the volume loss and the applied load.

The tests carried out in the tribometer to fit the wear model as well as that one carried out to validate it require long travel distances in a large number of cycles and consequently very long testing times. For instance, a test of 1000m, consisting of more than 21000 cycles, would require, with the model built for the friction law fitting, a calculation time for the finite element model of more than three months in a double CPU Intel Xeon Quad-core server at 2.66 GHz and 32Gb RAM. Therefore, to simulate the wear process involving long travel distances, it is necessary to set up a procedure to simulate an accelerated wear process. The fitting of the procedure is carried out by means of finite

element simulations of the TPU pad wear process with the 3D model set up in the TPU specimen-counterpart friction law fitting. The model considers the same assumptions as those explained previously and is fed with the friction curve resulting in its sixth iteration.

With the procedure detailed in section 3 applied to the case of external load of 75 N at 1000 m of travelled distance, the detailed description of the process and the results attained at each simulation are included in Table 3, while the evolution of the worn volume at the end of each simulation along the number of cycles is shown in Figure 16.

Table 3
Simulations considered in the fitting procedure development of an accelerated wear model

Divisions	*Subdivision*	*Cycles*	*Distance (m)*	*α equivalent*	*Worn volume (mm^3)*	*Diff. with mean exp value**
1	1	1	1000	75000	6.567	0.092
2	1	2	250	18750	6.956	0.157
	2	1	500	37500		
3	1	4	83.33	6250	7.016	0.167
	2	2	166.67	12500		
	3	1	333.33	25000		
4	1	8	31.25	2343.75	7.036	0.17
	2	4	62.5	4687.5		
	3	2	125	9375		
	4	1	250	18750		
5	1	16	12.5	937.5	7.025	0.168
	2	8	25	1875		
	3	4	50	3750		
	4	2	100	7500		
	5	1	200	15000		
6	1	32	5.21	390.63	6.972	0.16
	2	16	10.42	781.25		
	3	8	20.83	1562.5		
	4	4	41.67	3125		
	5	2	83.33	6250		
	6	1	166.67	12500		
7	1	64	2.23	167.41	6.905	0.148
	2	32	4.46	334.82		
	3	16	8.93	669.64		
	4	8	17.86	1339.29		
	5	4	35.71	2678.57		
	6	2	71.43	5357.14		
	7	1	142.86	10714.29		
8	1	128	0.98	73.24	6.778	0.127
	2	64	1.95	146.48		
	3	32	3.91	292.97		
	4	16	7.81	585.94		
	5	8	15.63	1171.88		
	6	4	31.25	2343.75		
	7	2	62.5	4687.5		
	8	1	125	9375		
9	1	256	0.43	32.55	6.568	0.092
	2	128	0.87	65.1		
	3	64	1.74	130.21		
	4	32	3.47	260.42		
	5	16	6.94	520.83		
	6	8	13.89	1041.67		
	7	4	27.78	2083.33		
	8	2	55.56	4166.67		
	9	1	111.11	8333.33		
10	1	512	0.20	14.65	6.048	0.006
	2	256	0.39	29.3		
	3	128	0.78	58.59		
	4	64	1.56	117.19		
	5	32	3.13	234.38		
	6	16	6.25	468.75		
	7	8	12.5	937.5		
	8	4	25	1875		
	9	2	50	3750		
	10	1	100	7500		

***The deviation is defined as:** $\dfrac{\left|W_{num} - W_{\exp}\right|}{W_{\exp}}$

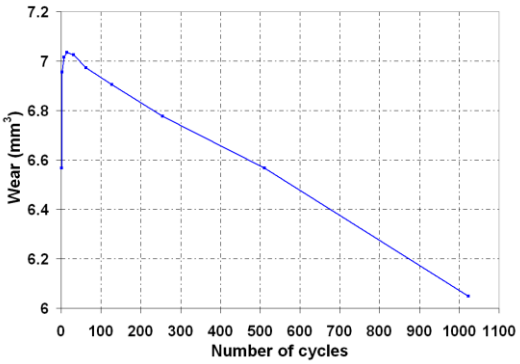

Figure 16. Evolution of the worn volume along the number of cycles.

Figure 17 and Figure 18 show the evolution of the wear and the maximum contact pressure attained in the specimen-counterpart contact pair along the travelled distance respectively for the several simulations carried out, while Figure 19 shows the wear distributions in height units at the end of the simulations with 1, 4, 7 and 10 divisions.

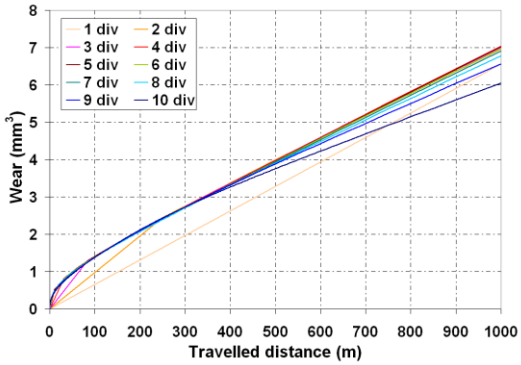

Figure 17. Evolution of the wear curves along the travelled distance.

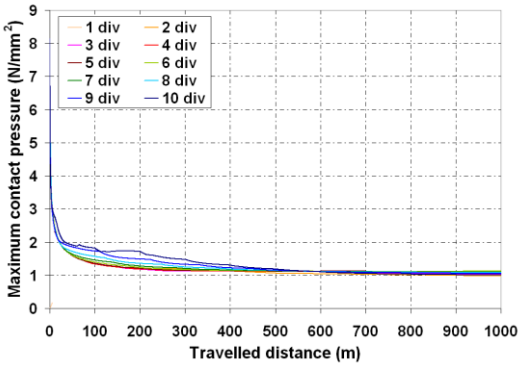

Figure 18. Evolution of the maximum contact pressure along the travelled distance.

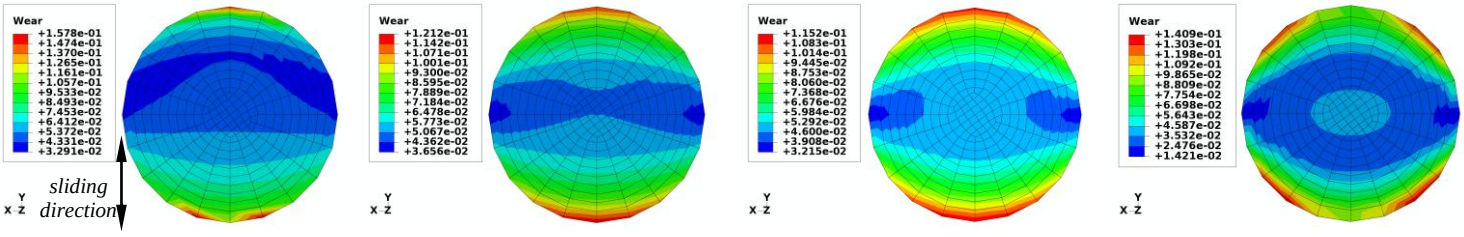

(a). Distribution of wear for simulation with 1 division.

(b). Distribution of wear for simulation with 4 divisions.

(c). Distribution of wear for simulation with 7 divisions.

(d). Distribution of wear for simulation with 10 divisions.

Figure 19. Wear distribution for different simulations.

According to the results shown in Figure 17, the initial part of the curve, the first 100 m of travelled distance, can be identified as the running-in stage of the wear curve. The stationary stage starts at a travelled distance of 200 m, where a rough constant slope is attained [1][26]. To confirm this trend, the evolution of the maximum contact pressures in Figure 18 shows an abrupt decrease for travelled distances lower than 100 m and an almost constant behaviour conserved from that distance. Moreover, according to the evolution of the wear distribution shown in Figure 19, the maximum wear is located at the top and bottom parts of the specimen, with non-symmetric distributions for simulations from 1 to 4 divisions, possibly because the running-in stage is covered by too few steps in those simulations. Regarding the evolution of the worn volume over the number of divisions in the simulation and with

regard to the experimental results, shown in Figure 16, the deviation increases up to 15 cycles, decreasing from that point and attaining differences lower than 10% from simulations with 500 cycles, those of 9 and 10 divisions. In any event, the results up to 4 divisions are managed with an insufficient number of steps in the running-in stage, the zone with the highest wear rate variation. Therefore, it is necessary to consider a number of steps in the running-in stage corresponding at least to the simulation with 15 cycles.

According to these results, the evolution of the wear curve is highly dependent on reproducing accurately the running-in zone where the highest wear rate variation takes place. However, the values attained experimentally in this part of the curve are significantly lower that those obtained at the distances at which the weight loss is measured. It is therefore not critical to obtain the weight loss at the running-in stage to obtain the wear model. Besides, this zone cannot be reproduced accurately enough in the tests because the values are within the scatter of the experimental measurements.

The importance of updating the geometry after applying the wear model by means of the user subroutine and the adaptive mesh technique in the wear results can be appreciated in Figure 20. The wear value obtained in the simulation of one cycle considering the model constants according to the real wear (α=3.45) is extrapolated to 1000 m, corresponding to a case without an updated geometry, obtaining 389 mm^3 of worn volume instead of 7.036 mm^3 obtained, for instance, for the simulation with 4 divisions.

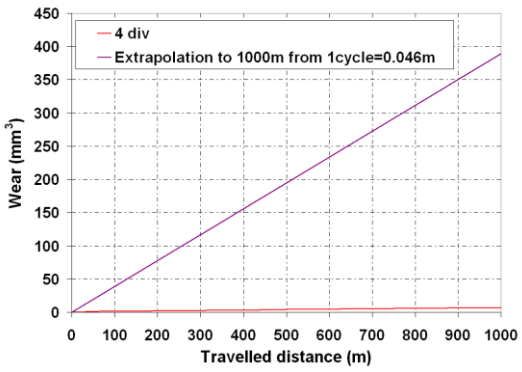

Figure 20. Evolution of the wear extrapolating values from 1 cycle up to 1000 m.

Analysis of the mesh size influence in the plane X-Y:

As the initial wear is clearly located at some specific points, this study is completed with an analysis of the mesh size influence in the plane *X-Y*. The results of the simulation with 4 divisions with the model described above are compared with those obtained with a model of 12267 nodes and 10240 elements with a finer mesh at the zones at which the highest wear values are obtained. The refined model has three elements to every one element of the coarse model in the radial direction and nine elements to every one in the tangential direction. Figure 21 shows a comparison of both models.

(a). Model with coarse size mesh in plane *X-Y*.

(b). Model with fine size mesh in plane *X-Y*.

Figure 21. Mesh comparison in analysis of mesh size influence.

Figure 22 shows the evolution of the wear along the travelled distance for both models, while Figure 23 shows the wear distribution for the model with finer mesh in the plane *X-Y*. This result can be compared with that shown in Figure 19 (d).

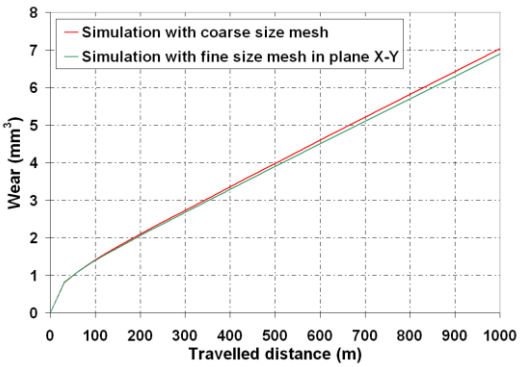

Figure 22. Evolution of wear curves for simulation with 4 divisions. Analysis of mesh influence in plane *X-Y*.

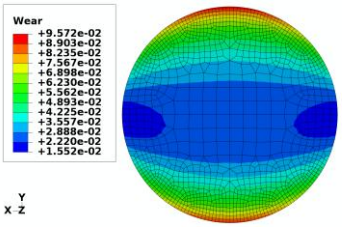

Figure 23. Wear distribution for simulation with fine mesh in plane X-Y. Simulation with 4 divisions.

A comparison of the two sets of results shows a maximum difference in the wear evolution curve of 2.6%, with a similar trend in both cases. The methodology can therefore be said to be independent of the model meshing bearing in mind that the mesh distribution has a minimum level of detail to capture the changes of the contact pressure distribution. It achieves a stationary wear stage and represents a compromise between the accuracy of the results and the computational cost. The simulation with the coarse mesh is around 12 times faster than the simulation with the fine mesh model, with differences in predicted wear below 5%.

Analysis of the mesh size influence in direction Z:

The influence of the mesh height in the adaptive mesh zone has also been studied. A simulation of the case with four divisions and finer mesh in direction *Z* was carried out in a model with 3525 nodes and 3136 elements. The refined model has three elements to every one element of the coarse model in the zone closest to the counterpart. Figure 24 shows a comparison of both models.

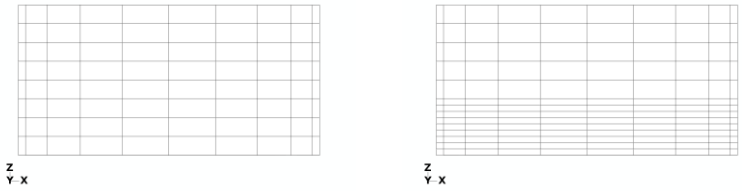

(a). Model with coarse size mesh in direction Z.

(b). Model with fine size mesh in direction Z.

Figure 24. Mesh comparison in analysis of mesh size influence.

Figure 25 shows the evolution of the wear along the travelled distance for both models, while Figure 26 shows the wear distribution for the model with finer mesh in direction *Z*. This result can be compared with that shown in Figure 19 (d).

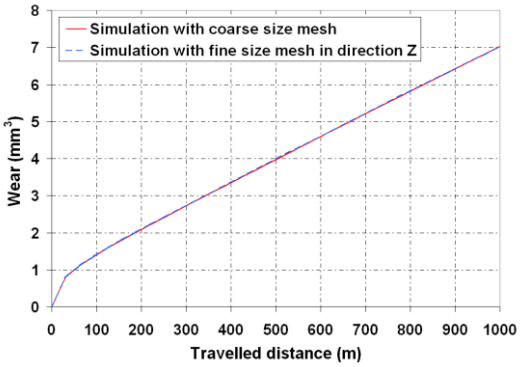

Figure 25. Evolution of wear curves for simulation with 4 divisions. Analysis of mesh influence in direction *Z*.

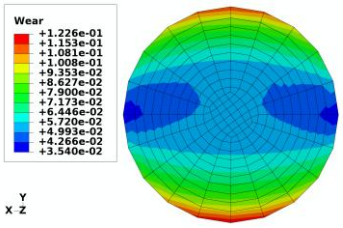

Figure 26. Wear distribution for simulation with fine mesh in direction *Z*. Simulation with 4 divisions.

A comparison of the two sets of results reveals that the maximum difference in the wear evolution curve is lower than 0.5%, showing a similar trend in both cases. It can therefore be asserted that the meshing criteria considered for the coarse mesh is sufficiently accurate for simulating the wear process in this study.

Analysis of the TPU material:

Although the previous analyses have been carried out considering TPU as a linear elastic material, the influence of the material plasticity has also been established. The results are compared of the same simulation with four divisions considering the TPU as a linear elastic material and considering it to be elastoplastic [33][34]. Figure 27 shows the material curve obtained from the compression characterisation test and that obtained when considering TPU as a linear elastic material.

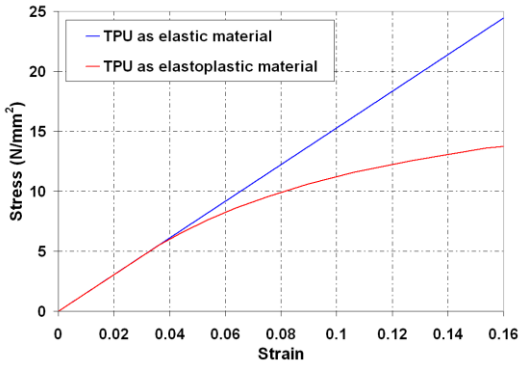

Figure 27. TPU curves considered as linear elastic and elastoplastic material.

Figure 28 shows the evolution of the wear along the travelled distance for both simulations, while Figure 29 shows the wear distribution for the simulation with TPU as an elastoplastic material. This result can be compared with that shown in Figure 19 (d).

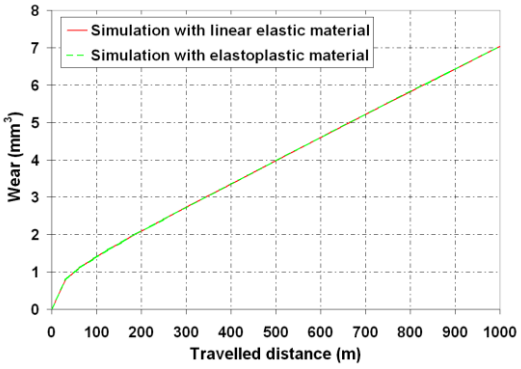

Figure 28. Evolution of wear curves for simulation with 4 divisions. Analysis of TPU material.

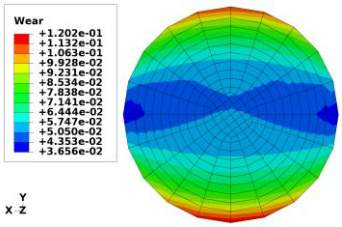

Figure 29. Wear distribution for simulation with TPU as elastoplastic material. Simulation with 4 divisions.

A comparison of both sets of results shows a maximum difference in the wear evolution curve of lower than 0.5%, showing a similar trend in both cases. It is therefore clear that the results obtained considering the TPU as a linear elastic material are sufficiently accurate.

4.3. Validation of the wear simulation procedure. Simulation of wear test under new conditions

A new 3D finite element model has been built in order to reproduce the same experimental conditions set up in the wear model validation tribotests, described in section 2.2. The parts considered are the TPU pad and encapsulating tool, both considered as deformable bodies, and the counterpart, considered as an analytical rigid surface. A scheme of the model with the parts involved is shown in Figure 7. Figure 30 shows an image of the model.

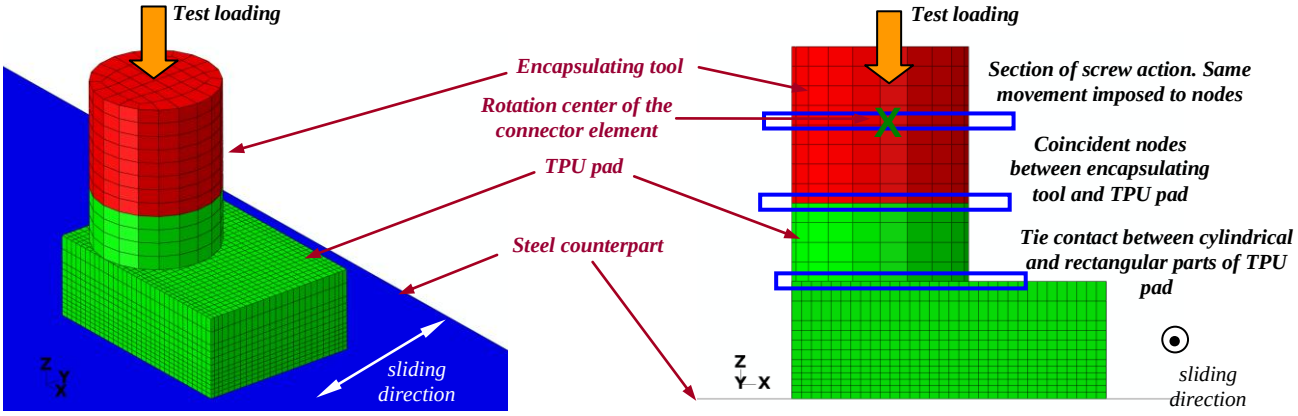

Figure 30. Finite element model of the validation wear tribotests.

The interaction between the TPU specimen and the encapsulating tool is modelled by means of coincident nodes in the contact surface, while the fixing of the whole pin to the machine frame is modelled by imposing the same movement on the section nodes of the encapsulating tool where the load is applied, in all the degrees of freedom. On the other hand, a dissimilar mesh is used in the cylindrical and rectangular parts of the TPU pad in order to reduce the model size. To link the movement of both parts, and considering that this is not a zone under analysis, a tied contact is defined between them. Unlike the conditions set up between the whole pin and the machine frame in the tests to fit the wear model, where the load is centred on the specimen, the tolerances between both parts can allow a relative rotation between them during the test, helped by the load eccentricity effect. According to the tolerances of the parts in the tests and the location where the screw acts, an estimated maximum relative rotation of 7.5º in direction "X" between both bodies is allowed. The external load acts over the whole pin in

direction "-Z", while the sliding direction acts in direction "Y". The connector definition and the load and displacement applications are placed at the central node of the encapsulating tool section where the screw acts.

The geometry and meshing of the model is carried out using the I-DEAS code, while the software used in the calculations is Abaqus/Standard-v6.8. The model consists of 11869 nodes and 10128 elements.

The TPU material properties of the pad are the same as those used in the simulations of the friction and wear model fittings: linear elastic material of elastic modulus 150 MPa, with a Poisson's coefficient of 0.35. The encapsulating tool is modelled as steel, with linear elastic material of elastic modulus $2.1 \cdot 10^5$ MPa and Poisson's coefficient of 0.29. The interaction between the TPU and the countermaterial is defined by the friction model obtained in the sixth iteration of the fitting of section 3.2. According to the conclusions extracted from the accelerated numerical modelling of the wear process detailed in section 4, the highest variation in the wear rate takes place for the first 100 m of travelled distance. In order to reproduce the wear process more accurately at the beginning of the curve, and considering a suitable number of steps for the model size to be able to run the simulation in an affordable computational time, ten cycles are simulated up to 100 m and nine cycles from 100 m to 1000m, all of them at 75 N of applied load. Table 4 shows a description of the variables involved in the simulation and the corresponding results attained, together with a comparison with the experimental test. The evolution of the wear and the maximum contact pressure attained in the specimen-counterpart contact pair along the travelled distance and the wear distribution and deformed shape of the specimen at the end of the simulation are shown in Figure 31 to Figure 34.

Table 4

Description of the simulation of the wear test under new conditions

Number of divisions	*Subdivision*	*Number of cycles*	*Distance (m)*	*α equivalent*	*Worn volume (mm^3)*	*Difference with regard to mean exp value**
1	1	10	100	750	29.307	0.146
	2	9	900	7500		

***The deviation is defined as:** $\dfrac{|W_{num} - W_{\exp}|}{W_{\exp}}$

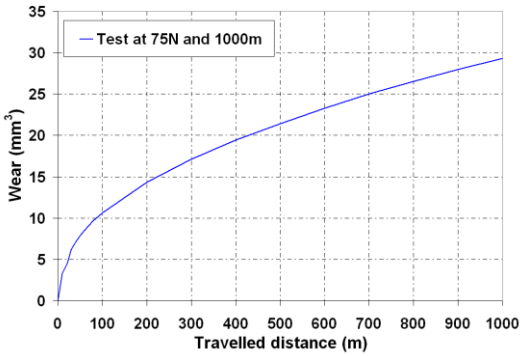

Figure 31. Evolution of the wear curve along the travelled distance for the simulation of the wear model validation.

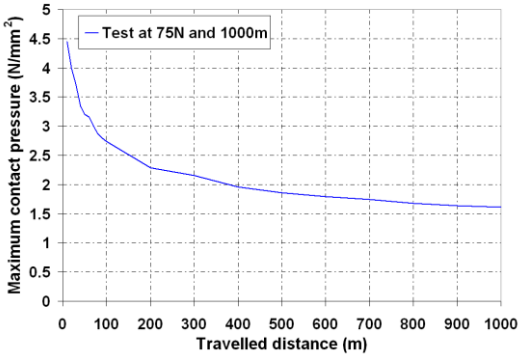

Figure 32. Evolution of the maximum contact pressure curve along the travelled distance for the simulation of the wear model validation.

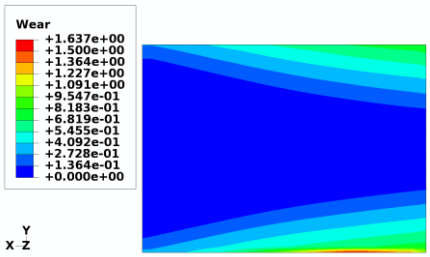

Figure 33. Wear distribution (mm) for simulation of wear test under new conditions.

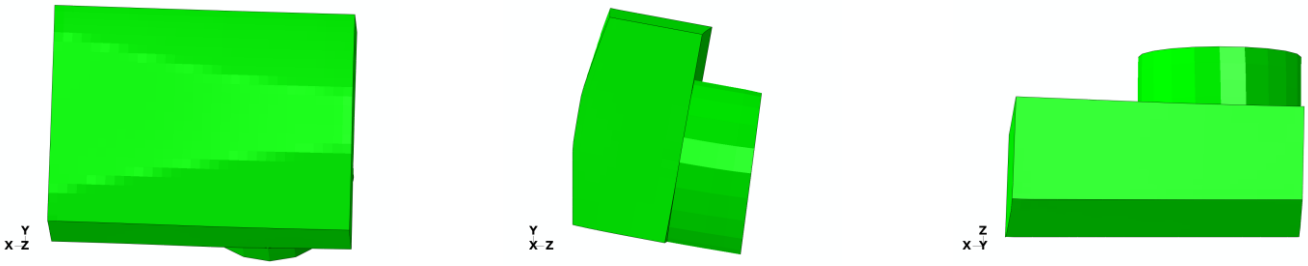

Figure 34. Specimen deformed shape for simulation of wear test under new conditions.

According to the results shown in Figure 31, the initial part of the curve shows the highest variation in the wear rate, an effect which can be corroborated with the highest variation of the maximum contact pressure in Figure 32. Unlike the wear curve attained in the accelerated numerical modelling of the wear process, shown in Figure 18, the wear rate variation is still significant after the first 100 m. This behaviour can be explained by the deformed shapes of the specimen shown in Figure 34, where the wear is not uniform over the whole specimen surface due to the load eccentricity. On the other hand, comparing these deformed shapes of the specimen with the images of the worn specimens after the tests, shown in Figure 8, a good qualitative numerical-experimental agreement is obtained, showing similar specimen shapes after being worn and attaining in both cases the maximum wear at the zone where the load is applied.

The importance of updating the geometry after applying the wear model by means of the user subroutine and the adaptive mesh technique in the wear results can be appreciated again in Figure 34, where an important change in the geometry of the deformed model with regard to the initial undeformed model is shown.

On the other hand, the evolution of the wear curve in Figure 31 shows a more significant running-in than in the simulation of the wear process carried out to fit the wear model, tested with a centred load. This result confirms that the wear rate change in the running-in zone is more important in cases with geometric modification of the specimen during the wear test caused by effects such as the high friction coefficient in the contact pair and, as in this case, the load eccentricity.

5. Conclusions

This work describes a methodology to numerically model the friction wear phenomena in a polymer-steel contact pair, which reproduces the contact in an industrial component between a guide shoe insert, made of TPU, and the corresponding guide, made of steel. It also describes the implementation of the model in the general purpose commercial finite element code Abaqus. The wear model is obtained from data fitting of wear tribotests. The numerical implementation combines three main aspects: implementation of the wear model via a user subroutine with the application of the adaptive meshing technique, numerical characterisation of a friction law dependent on the contact pressure and setting up a procedure to numerically accelerate the wear simulation.

Regarding the wear model characterisation from tribotests, a power law relationship is established between the volume loss and the applied load, and subsequently the contact pressure, contradicting what is stated by Archard's law in which it is stated that this relationship is linear. This fact is corroborated by results from tribotests.

Regarding the first procedure developed in the general methodology to implement a wear model in a finite element code, by means of the user subroutine Umeshmotion, different routines to result access, and using the adaptive meshing technique, the usefulness and capacity of finite element simulations to solve this type of problems have been demonstrated, taking into consideration some particularities in its numerical implementation, such as a particular order of the mesh numeration, the definition of the wear direction in singular zones of the model, edges and corners, and the implementation of the wear distribution maps, not directly available in Abaqus.

In the second numerical procedure developed in the methodology to implement a wear model, for obtaining a TPU-steel friction law, an iterative process based on a fixed-point method has been carried out, been applied to the results of finite element simulation of one cycle of the wear tribometer tests, obtaining a convergence in a reasonable number of iterations.

In the third numerical procedure set up to implement the wear model in an accelerated way, procedure based on a politomic division method, different conclusions arisen from this study. In all the cases, the wear evolution is directly related with the maximum contact pressure distribution. Initially, the high deformation of the specimen, caused by the high friction between the parts in contact, implies a sharp change in the contact pressure distribution, a geometric modification of the specimen and a non-uniform wear in the contact surface up to the contact pressure distribution is uniform. The highest wear in the specimen is produced in the part with highest friction and highest contact pressure distribution is attained. According to the politomic division method, the complete evolution of the wear curve numerically obtained is highly dependent on the accurate reproduction of the initial running-in stage, where a highest variation in the wear curve takes place, being recommended to consider the highest number of cycles in the initial wear curve. With this procedure, although there is some influence of the number of divisions on the wear results, attaining differences up to 15% with regard to the experimental results and showing differences in the wear distribution maps, a good approximation is obtained with a significant reduction in the number of test cycles simulated and thus a reduction in the calculation time. Besides, this procedure allows the different stages of a typical wear curve, the initial running-in stage as well as the stationary one, to be obtained accurately.

The methodology of the wear process implementation presented in the current work is validated with its application to a problem with geometry and working conditions different to those used to implement the wear process, obtaining accurate results from qualitative and quantitative points of view, with differences of around 15% with regard to the experimental results. This validation also shows the importance of updating the geometry after applying the wear model by means of the user subroutine and the adaptive mesh technique in the wear results is also appreciated. In this particular case, the mesh distribution of the specimen, taking into account a minimum level of detail to capture the changes in the contact pressure distribution, has low influence in the results. Besides, in this particular case also, the fact of considering TPU material as linear elastic is approximated enough to set up the numerical methodology to implement the TPU-steel wear model.

The limitations arising from this study relate, on the one hand, to the adaptive meshing technique. The use of this technique recommends consideration of the material properties as linear elastic due to the inaccurate use of the adaptive mesh technique with hyperelastic material models. A further extension of the current work would be to analyse the accuracy of this methodology for other polymers with a more significant non-linear behaviour than TPU. On the other hand, the wear model implemented in this work could be extended by including other dependencies such as the temperature or the countersurface roughness. In any case, both variables are controlled throughout the tests in order to assure their repeatability and their dependency is implicitly included in the wear model constants way.

Other future actions already planned by the research group relate to the application and validation of the wear model as well as of the methodology followed in order to numerically implement it to the guide shoe insert component under real working conditions, to carry out an extension of the methodology under lubricated test conditions, and to develop a more precise method to measure the wear of the specimen at the beginning of the test reproducing the wear curve accurately in the running-in stage.

Acknowledgements

This work is included within the framework of the European project "Kristal" (Knowledge-based Radical Innovation Surfacing Tribology and Advanced Lubrication, contract Nr.: NMP3-CT-2005-515837).

References

[1] S.W. Zhang, Tribology of Elastomers, Tribology and interface engineering series, NO. 47, B.J. Briscoe, 2004, pp, 37, 177.

[2] M.J. Neale and M. Gee, Guide to wear problems and testing for industry, New York, USA, William Andrew Publishing; 2001.

[3] X. Jia and R. Ling, Two-body free-abrasive wear of polyethylene, nylon1010, expoxy and polyurethane coatings, Tribology International 40(8) (2007) 1276-1283.

[4] H.C. Meng, K.C. Ludema, Wear models and predictive equations: their forma and content, Wear 181-183 (1995) 443-457.

[5] J.F. Archard, Contact and rubbing of flat surfaces, J. Appl. Phys., 24 (1953) 981-988.

[6] I.M. Hutchings, "Friction and Wear of Engineering Materials", Ed. Edward Arnold, a Division of Hodder Headline PLC, 1992.

[7] D. Giraldo, J.M. Veléz, "Estudio del desgaste por deslizamiento en seco de algunos plásticos", Revista Dyna, Medellín, 136 (2002) 11-20.

[8] R. Liu, D.Y. Li, "Modification of Archard's equation by taking account of elastic/pseudoelastic properties of materials", Wear, 251 (2001) 956-964.

[9] J.F. Molinari, M. Ortiz, R. Radovitzky, E.A. Repetto, "Finite element modeling of dry sliding wear in metals", Eng. Comput., 18 (2001) 592-609.

[10] A.A. Torrance, A method for calculating boundary friction and wear, Wear 258 (2005) 924-934.

[11] A. Cantizano, A. Carnicero and G. Zavarise, Numerical simulation of wear-mechanism maps, Computational Materials Science 25 (2002) 54-60.

[12] V. Hegadekatte, N. Huber, O. Kraft, Finite element based simulation of dry sliding wear, Modelling and Simulation in Materials Science and Engineering 13 (2005) 57-75.

[13] V. Hegadekatte, S. Kurzenhäuser, N. Huber, O. Kraft, A predictive modeling scheme for wear in tribometers, Tribology International 41 (2008) 1020-1031.

[14] S. Mukras, N. H. Kim, W.G. Sawyer, D.B. Jackson, L.W. Bergquist, Numerical integration schemes and parallel computation for wear prediction using finite element method, Wear 266 (2009) 822-831.

[15] S. Bouissou, J.P. Petit, M. Barquins, "Normal load, slip rate and roughness influence on the polymethylmethacrylate dynamics of sliding: 1. Stable sliding to stick-slip transition", Wear, 214 (1998) 156-164.

[16] F.J. Martínez, M. Canales, et al., Tribological behavior of thermoplastic polyurethane elastomers, Wear 268 (2010) 388-398.

[17] D.L. Burris and W.G. Sawyer, A low friction and ultra low wear rate PEEK/PTFE composite, Wear 261 (2006) 410-418.

[18] J. Song, P. Liu, M. Cremens and P. Bonutti, Effects of machining on tribological behavior of ultra high molecular weight polyethylene (UHMWPE) under dry reciprocating sliding, Wear 225-229 (1999) 716-723.

[19] S.E. Franklin, Wear experiments with selected engineering polymers and polymer composites under dry reciprocating sliding conditions, Wear 251 (2001) 1591-1598.

[20] D.K. Baek and M.M. Khonsari, Friction and wear of a rubber coating in fretting, Wear 258 (2005) 898-905.

[21] N.P. Suh, M. Mosleh and J. Arinez, Tribology of polyethylene homocomposites, Wear 214 (1998) 231-236.

[22] J.J. Liu, P.A. Zhou, X.T. Sun, Q.C. Liao, el at., Adhesive wear and fatigue wear of materials, Beijing: Machinery Industry Press (1989) 234-323.

[23] J. Yi, M.C. Boyce, G.F. Lee, E. Balizer, Large deformation rate-dependent stress-strain behaviour of polyurea and polyurethanes, Polymer, 47 (2006) 319-329.

[24] S.S. Sarva, S. Deschanel, M.C. Boyce, W. Chen, Stress-strain behavior of a polyurea and a polyurethane fron low to high strain rate, Polymer 48 (2007) 2208-2213.

[25] A.G. Thomas, J. Polym. Sci. Symp., 48 (1974) 145.

[26] K. Cho, D. Lee, "Effect of molecular weight between cross-links on the abrasion behaviour of rubber by a blade abrader", Polymer, 41 (1) (2000) 133-140.

[27] A. Schallamach, Friction and abrasion of rubber. Wear, 1 (1958) 384-417.

[28] A.M. Harder, "Fixed point theory and stability results for fixed point iteration procedures", Ph.D. thesis, University of Missouri-Rolla, 1987.

[29] J. Biazar, A. Amirteimoori, "An improvement to the fixed point iterative method", Applied mathematics and computation, 182 (2006) 567-571.

[30] M.A. Jiménez, J.M. Bielsa et al., The influence of the contact pressure on the dynamic friction coefficient in cylindrical rubber-metal contact geometries, IUTAM Symposium on Computational Methods in Contact Mechanics (2006) 257-275.

[31] J. Bentley, "Programming pearls (2nd edition)", 34, 2000.

[32] T.H. Cormen, C.E. Leiserson, R.L. Rivest, C. Stein, "Introduction to algorithms", MIT Press, 2000.

[33] ASTM D638 "Standart Test Method for Tensile Properties of Plastics".

[34] ASTM D695 "Standart Test Method for Compressive Properties of Rigid Plastics".

[35] R. Elleuch, K. Elleuch, et al., Tribological behavior of thermoplastic polyurethane elastomers, Materials & Design 28(3) (2007) 824-830.

[36] R.C.L. da Silva, C.H. da Silva, et al., Is there delamination wear in polyurethane?, Wear 263(7-12) (2007) 974-983.